Point Defects and Impurities in Silicon Carbide and Group III-Nitrides☆

Piotr Bogusławski, Instytut Fizyki PAN, Warsaw, Poland
Jerry Bernholc, North Carolina State University, Raleigh, NC, United States
Shanmugasundaram Sivarajan, VIT University, Chennai, India

Group III nitrides and SiC are perhaps the most important materials to emerge for use in optoelectronic, high-speed, and high-temperature devices. Owing to the presence of first-row elements, nitrogen and carbon, some of their physical properties differ significantly from those of classical semiconductors such as GaAs or silicon. The bond strengths of these materials are very high, leading to high melting temperatures, slow diffusion of substitutional defects and impurities, and difficulties in growth and annealing. However, the high bond strengths prevent material degradation; the optoelectronic devices operate successfully with defect densities that would be unthinkable in traditional semiconductors.

Most of the device applications of semiconductors require controlled doping. In wide-bandgap nitrides the doping efficiency is lower than in typical III–V compounds, owing to higher ionization energies of shallow impurities. For example, the ionization energies in GaAs and in GaN are 6 meV and 32 meV, respectively. This stems from higher effective masses of carriers and lower dielectric constants in wide-bandgap semiconductors. Consequently, electrical characteristics of devices may sometimes be better at high temperatures than at room temperature, since more dopants are ionized. Additional factors controlling the doping efficiency are the mode of incorporation and the presence of native defects.

If the dopants are introduced during growth or by in-diffusion, their solubility determines the maximum dopant incorporation. However, native point defects, which as a rule are electrically active, may form to compensate for the doping. The energetic gain of compensating, for example, a donor with an acceptor, increases with the size of the bandgap. Such effects are important in wide-gap materials, because the energetic gain of compensating, for example, a donor with an acceptor increases with the size of the band gap. In group III nitrides it is believed that cation vacancies or their complexes compensate donors and lead to the so-called yellow luminescence, while the nitrogen vacancy is probably the most important compensating donor. Furthermore, since the formation energies and thus the concentrations of native defects depend on the position of the Fermi level, an increased number of electrically active dopants increases the propensity to form compensating native defects, leading to a reduction in doping efficiency.

Ion implantation is not limited by solubility, nor is it affected by low diffusivities. This is the most important way of doping SiC wafers, since thermal diffusion is precluded owing to the low diffusivities of dopants at temperatures lower than 1000°C. However, the process of implantation creates native defects and their complexes, e.g., divacancies and vacancy–interstitial (Frenkel) pairs, which change crystal properties and cause degradation of sample quality. It is thus important both to understand properties of native defects and to establish annealing procedures that lead to device-quality material. The type of the dominant irradiation-induced defect depends on several factors, such as the type of irradiating particles (electrons, neutrons, dopant atoms), their energy, fluence, and sample temperature during implantation. In lightly irradiated samples, vacancies and interstitials are the main defects. At higher fluences, vacancies may recombine with interstitials and create antisites. Defect complexes may also form and the near-surface region may become amorphous. Regardless of the reasons for their formation, native defects can degrade the device characteristics by acting as recombination centers.

☆*Change History*: June 2017. Shanmugasundaram Sivarajan added an Abstract, Keywords; updated the text with additional review materials and updated the list of references.

 doi:10.1016/B978-0-12-803581-8.03181-7

The properties of native point defects in SiC and group III nitrides are first discussed. Experimentally, these are the only point defects that have been clearly identified in both materials. Theoretical results concerning interstitials and antisites are also summarized. Experimental studies of defect annealing in SiC are also discussed. While good *n*- and *p*-type dopants for SiC have been identified, the situation in group III nitrides is significantly more complex. The focus is here on doping with group IV impurities, for which self-compensation effects on doping efficiency need to be considered, and on selenium, for which compensation by native defects has been observed. The final section discusses briefly interfacial segregation in heterostructures (accumulation of dopants and defects in one of the components of the heterostructure). The results indicate that this effect is of greater importance in nitrides than in classical semiconductors.

1 Theoretical Background

Ab initio methods provide accurate results for the total energy of a solid (with or without defects). This allows one to compute the highest possible concentration of an impurity (called the solubility limit) of a defect at thermodynamic equilibrium, which is given by

$$[\mathrm{conc}] = \mathrm{N_{sites}}\exp(\mathrm{S_{form}}/\mathrm{k_B} - \mathrm{E_{form}}/\mathrm{k_B T}) \tag{1}$$

where N_{sites} is the concentration of atomic sites on which the defect or the dopant may reside, and E_{form} and S_{form} are its formation energy and entropy, respectively. Since E_{form} is of the order of 1 eV or more and S_{form} is typically about $4–8k_{\mathrm{B}}$, the latter can usually be neglected. The formation energy of, e.g., $\mathrm{Si_{Ga}}$ in GaN in a charge state q is

$$\mathrm{E_{form}(q)} = \mathrm{E_{tot}(GaN : S_{Ga})} - \mathrm{E_{tot}(GaN)} + \mu_{\mathrm{Ga}} - \mu_{\mathrm{Si}} + \mathrm{qE_F} \tag{2}$$

where E_{tot} is the total energy of the crystal with or without the impurity, μ are the chemical potentials of the sources of atoms, and E_{F} is the Fermi energy. The actual experimental conditions determine the chemical potentials of the sources of atoms involved in doping, and thus the formation energy and the solubility limit. Eqs. (1) and (2) also give the concentrations of native defects. One should note, however, that the concentrations correspond to the growth temperature and not room temperature. Furthermore, if the growth occurs faster than the equilibrating diffusion, it is possible to "freeze" the defect or dopant concentration that reflects the near-surface formation energies, which can be significantly different from the bulk.

In the case of charged impurities and defects, formation energies are in general reduced by electron transfer to/from the Fermi level according to Eq. (2). This increases their concentrations according to Eq. (1). Since the energy gain may be of the order of the bandgap, the formation of charged defects and impurities is of particular importance in wide-bandgap materials (Boguslławski *et al.*, 1995).

Eqs. (1) and (2) show that the concentration of dopants and native defects are inter-related: introduction of dopants into the crystal influences the position of the Fermi level and thus E_{form} of native defects. The Fermi level is to be determined self-consistently together with the concentrations of dopants and defects, from the condition that the crystal is electrically neutral. In particular, these equations describe the reduction of doping efficiency owing to compensation: doping with donors reduces the formation energy of acceptors, which leads to an increase of their concentration and thus compensation of doping. In an analogous way, donors compensate *p*-type dopants. The compensating donors and acceptors may be native defects, as is generally the case, or dopants – which is characteristic for the group IV impurities considered here.

In general, a group IV atom is likely to become a donor when incorporated on the cation site, and an acceptor on the anion site. Thus, a problem inherent to doping with group IV elements is self-compensation, i.e., simultaneous incorporation of the dopant on both cation and anion sublattices. In GaN and AlN compounds, where there are large differences between the atomic radii of cations and anions, self-compensation is blocked to some extent by strain effects. For example, a carbon atom in GaN should substitute for nitrogen, since the two atoms have similar atomic radii, while the substitution for the much bigger gallium induces a lattice strain energy of a few eV. However, in competition with the strain effects are processes of electron transfer from donors to acceptors. Owing to the wide bandgap of nitrides, they lead to large energy gains and thus enhance self-compensation. For the group IV dopants, the electron transfer effects may overcome the strain-driven preference of the dopant atom X to substitute for the component of a similar size, rendering formation energies of $\mathrm{X_{cation}}$ and $\mathrm{X_N}$ close to each other. Consequently, a simultaneous incorporation of X on both sublattices becomes possible. The degree of self-compensation strongly depends on the conditions of growth, and may vary from none to total self-compensation.

The tendency towards self-compensation is further increased by the formation of nearest-neighbor (NN) donor–acceptor pairs. The binding energy, E_{pair}, of group IV NN pairs in GaN and AlN is about 1 eV, and their formation energy is

$$\mathrm{E_{form}(XX)} = \mathrm{E_{form}}\left(\mathrm{X^{+}_{cation}}\right) + \mathrm{E_{form}}\left(\mathrm{X^{-}_{N}}\right) + \mathrm{E_{pair}} \tag{3}$$

which is independent of the Fermi level, E_{F}, for neutral pairs, i.e., for $E_{\mathrm{A}} < E_{\mathrm{F}} < E_{\mathrm{D}}$. The concentration of NN pairs is given by Eq. (1), with N_{sites} being four times larger than that for substitutional impurities. Thus, [XX] is comparable to $[\mathrm{X_{cation}}]$ or $[\mathrm{X_N}]$ only when the binding energy is similar to the formation energy of $\mathrm{X_N}$ or $\mathrm{X_{cation}}$, respectively.

Another channel quenching the doping efficiency is the stabilization of donors in DX-like configurations (Chadi and Chang, 1988). In this configuration a bond between the impurity and one of its first neighbors is broken, and one (or both) of these atoms move from their substitutional sites to interstitial locations. The transformation of the impurity to a DX configuration is commonly

accompanied by a capture of a second electron, which quenches the doping efficiency. An additional complication comes from the fact that in the wurtzite structure there are two nonequivalent DX configurations, in which the broken bond between the impurity and the host atom is either parallel (DX_1) or largely perpendicular (DX_2) to the *c*-axis. Their properties differ substantially in terms of stability and electronic structure, the DX_1 variant is less stable than DX_2 for C^-, and more stable for Si^- and Ge^-.

2 Vacancies

2.1 The Coulson Model

The electronic structure of vacancies in tetrahedrally bonded crystals is well described by the Coulson model. A vacancy, i.e., a removal of an atom, creates four dangling bonds with the nearest neighbors. The dangling bonds give rise to localized electronic states. In crystals with cubic symmetry, the appropriate combinations of these orbitals are the s-like singlet A_1 and the p-like triplet T_2, which is higher in energy than A_1. In most semiconductors, the A_1 state is a resonance degenerate with the continuum of the valence bands, while T_2 lies in the forbidden bandgap. The Coulson model also provides the electron occupations of the vacancy levels. For example, the silicon vacancy levels in cubic SiC are mostly formed from the four sp^3 orbitals of carbon. Each carbon atom has four valence electrons and thus contributes one electron to each bond. Consequently, there are four dangling-bond electrons, two of which occupy the A_1 singlet and the remaining two occupy the T_2 triplet. This holds both for carbon and silicon vacancies in their neutral charge states. Furthermore, the model correctly predicts that the T_2 state of the carbon vacancy (made out of silicon dangling bonds) is higher in energy than the T_2 state of the silicon vacancy (made out of carbon dangling bonds), since carbon is more electronegative than silicon and thus its orbitals are lower in energy. Similar arguments lead to the conclusion that the T_2 state of a cation vacancy in a cubic III–V compound is lower in energy than that of the anion vacancy, and that this state is occupied with three electrons and one electron for the neutral cation and anion vacancies, respectively.

In practice, several physical effects complicate the above picture. The detailed electronic structure of vacancies is determined by both the electron–electron and the electron–lattice interactions. Both factors may be important, since the dangling sp^3 bonds are fairly localized. First, the coupling with the lattice results in relaxation of atoms surrounding the defect. The amount and the symmetry of the atomic displacements depend on the charge state of the defect. In particular, when the ground state of the defect is an orbital singlet or a multiplet fully occupied with electrons, the atomic relaxation preserves the point group symmetry of the lattice and is of a "breathing mode" type. However, when the ground state of the defect is both degenerate and partially occupied by electrons, which is the case for vacancies in cubic crystals, the Jahn–Teller (JT) effect occurs, namely an atomic distortion that splits the degeneracy in such a way that the level(s) that are *lowered* in energy by the distortion are fully occupied, while those that move up are empty. The net effect is a lowering of the total energy and a less symmetric ground state.

In the absence of coupling with the lattice, or when this coupling is weaker than the electron–electron interaction, the effective interaction between the electrons is repulsive and the energy position of a level increases as a function of electron occupation. This situation is typical in III–V compounds and it also occurs for vacancies in group III nitrides. In this case, the electrons progressively occupy the T_2 state, which may accommodate up to six electrons. The consecutive electrons have alternating spins and therefore the total spin of the vacancy is either 0 or 1/2. In SiC, the actual structure of vacancies is more complex.

In crystals with hexagonal symmetry – lower than cubic – the T_2 triplet is split into a singlet and a doublet by the hexagonal crystal field. In the following, we refer to such singlet–doublet pairs as quasi-triplets. The splitting energies are in the range 0.1–0.7 eV.

2.2 Vacancies in SiC

The properties of V_{Si} and V_C in SiC are not typical when compared to other semiconductors. The silicon vacancy has been studied theoretically for both 3C- and 2H-SiC (Torpo *et al.*, 1999). In the case of V_{Si}, the spin–spin exchange interaction is larger than the JT spin–lattice interaction. For this reason, for V_{si}^- with three electrons in the T_2 level, the ground state is a high-spin configuration with $S=3/2$, which is a quartet $^4A_2$ – an orbital singlet not subject to the JT distortion. In the 3C polytype, this configuration is the ground state for Fermi energies ranging from 0.5 eV to 1.2 eV above the top of the valence bands. It is lower in energy by about 0.6 eV than the low-spin $S=1/2$ configuration. In the 2H polytype, the high-spin state is also found, but the vacancy levels are lower and the consecutive levels are more spread out in energy. The JT effect is weak. Comparable results for 3C-SiC have been obtained (Zywietz *et al.*, 1998). The formation energy of V_{Si} is about 7 eV (Wang *et al.*, 1988); this value is high and thus the equilibrium concentration of vacancies is expected to be very low.

These theoretical results agree well with experimental data. Experimentally, the silicon vacancy in *n*-type 3C-SiC was identified by Itoh *et al.* (1997). They demonstrated that the V_{si}^- is in the high-spin $S=1$ state with T_d symmetry (see **Fig. 1**). The vacancy-induced level is located at about 0.5 eV above the top of the valence bands. The same conclusions were reached by Wimbauer *et al.* (1997) for V_{si}^- in 4H-SiC, based on electron spin resonance (ESR) and electron nuclear double resonance. Their identification was based on the resolved hyperfine interactions with the carbon nearest and silicon second-nearest neighbors of the vacancy. Theoretical values of the hyperfine interaction constants (Wimbauer *et al.*, 1997) agree with the experimental data. The observed ESR signal is isotropic, and the ligand hyperfine interactions with silicon second-nearest neighbors are also isotropic. The magnetic resonance parameters obtained by the various groups for 3C, 4H, and 6H polytypes are almost identical.

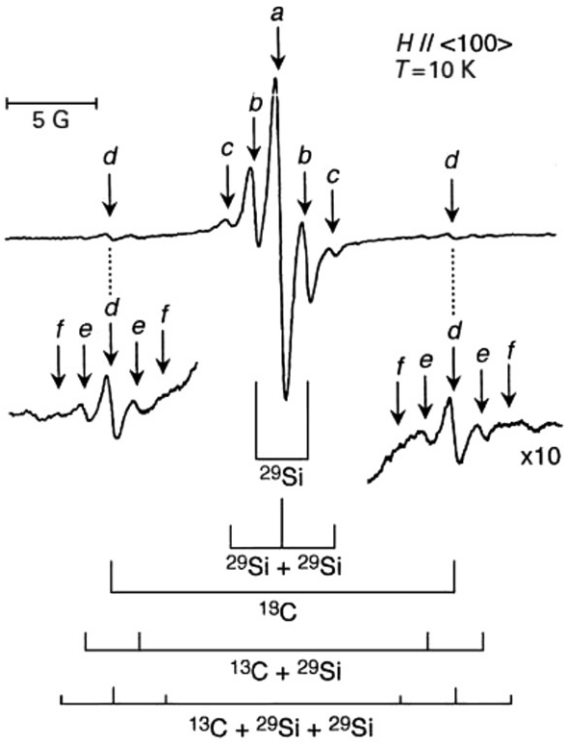

Fig. 1 ESR spectrum of a silicon vacancy for *n*-type 3C-SiC irradiated with protons. Hyperfine interactions with ^{13}C and ^{29}Si are also represented. After Itoh, H., Kawasuso, A., Ohshima,T., *et al.*, 1997. Intrinsic defects in cubic silicon carbide Phys. Status Solidi A 162, 73–198.

Turning to the carbon vacancy, theoretical calculations (Bechstedt *et al.*, 1998) for 3C-SiC reveal that the electron coupling with the lattice is strong and that the defect properties are dominated by a pronounced JT effect. Consequently, V_C exhibits the so-called negative-U behavior, described by the relationship

$$E_{tot}\left(V_C^{++}\right) + E_{tot}\left(V_C^{0}\right) < 2E_{tot}\left(V_C^{+}\right) \tag{4}$$

which shows that the $1+$ charge state is metastable. This situation may be described by the fact that for the V_C^+ effective electron–electron interaction is attractive. It is due to the very strong JT effect in the neutral charge state, which effectively lowers $E_{tot}(V_C^0)$, while for V_C^+ the JT effect is vanishingly small. The vacancy-induced levels are in the upper half of the bandgap, possibly close to the bottom of the conduction band. In the 4H polytype, these levels are lower in energy, as are the levels of V_{Si}. The difference between the nonequivalent (cubic and hexagonal) sites in 4H is typically 0.1–0.2 eV, which is a small fraction of the formation energy of about 4 eV. This is because these sites differ first in the configuration of their second neighbors. For comparison, the various nonequivalent sites in 6H-SiC are shown in **Fig. 2**. Turning to experiments, the V_C^+ was observed by Itoh *et al.* (1997) in cubic *p*-type samples. In agreement with theory – since it would only have one electron occupying the T_2 orbital – a JT distortion occurs and the symmetry is lowered from that of zinc blende to tetragonal.

It is interesting to note that the major properties of vacancies in SiC resemble those in pure end crystals: the vacancy in silicon is a negative-U defect, while the vacancy in diamond assumes the high-spin state. Correspondingly, V_C, which has silicon nearest neighbors, is a negative-U center, while V_{Si}, which has carbon nearest neighbors, has a high-spin ground state.

2.3 Vacancies in GaN, AlN, and AlGaN

We first consider *cation* vacancies. Since the formation of a cation vacancy creates dangling bonds on the four nitrogen neighbors, its levels should be close to the top of the valence band. Indeed, in GaN the quasi-triplet of a neutral V_{Ga} is located about 0.3 eV above the valence band edge and the hexagonal splitting is only 0.1 eV. Similar results are obtained for AlN. Since the quasi-triplet is populated with three electrons in the neutral charge state, V_{cation} can trap both electrons and holes. Recombination of electrons from the conduction band to the V_{Ga} levels can lead to the so-called yellow luminescence in group III nitrides.

Turning to the *nitrogen* vacancy, its electronic states are mainly composed of gallium dangling bonds. For this reason, the energy of the quasi-triplet is quite high. In GaN, the singlet state of the quasi-triplet is about 0.8 eV above the bottom of the conduction bands. The hexagonal splitting is 0.5 eV and this level contains one electron. However, since the quasi-triplet is a resonance, the electron autoionizes to the bottom of the conduction band, where it forms an effective mass state bound by the Coulomb tail of the vacancy potential. Consequently, V_N in GaN is a shallow donor, as confirmed by experiment (Look *et al.*, 1997). A similar level scheme holds for V_N in InN.

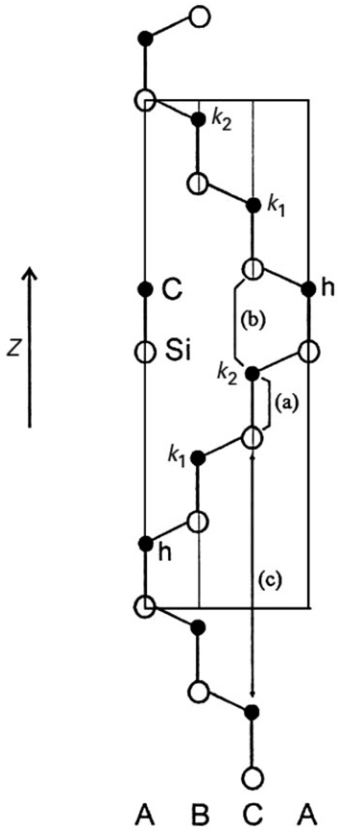

Fig. 2 Cross-section of the (1120) plane of a 6H-SiC unit cell, with a hexagonal (h) and two quasi-cubic (k_1 and k_2) sites. After Gruelich-Weber, S., 1997. EPR and ENDOR investigations of shallow impurities in SiC polytypes. Phys. Status Solidi ((a))95, 95–151.

The electronic structure of V_N in AlN is different, primarily due to the much wider bandgap of AlN. The energies of the vacancy-induced states relative to the top of the valence band are higher in AlN than in GaN, but the quasi-triplet is located below the bottom of the conduction band and V_N in AlN is a deep donor. Finally, the vacancy-induced symmetric A_1 level is inside the valence bands in both GaN and InN, but in AlN it is predicted to be a deep state at about 0.4 eV above the top of the valence bands.

The electronic structure of V_N in $Al_xGa_{1-x}N$ alloy cannot be obtained by a linear interpolation between the results for pure end compounds. This is due to a strong localization of vacancy-induced levels. In fact, the properties of vacancies are determined mainly by the chemical identity of the first cation neighbors (Boguslławski and Bernholc, 1999a). In $Al_xGa_{1-x}N$, there are five possible variants of V_N, which have $n=0, 1, \ldots 4$ gallium (or, equivalently, 4, 3, … 0 aluminum) neighbors, respectively. Theory indicates that the gallium-terminated variant is the lowest in energy, and therefore it is expected to occur more frequently than any other variant. The doping properties of V_N are determined by the position of the singlet level of this variant, which is shown in **Fig. 3**. We see that V_N is a shallow donor in $Al_xGa_{1-x}N$ for $x<0.5$ and a deep donor for higher compositions. All variants of V_N are compensating donors over the whole composition range.

3 Antisites and Interstitials

Antisites in 3C- and 2H-SiC have been studied theoretically by Wang *et al.* (1988) and Torpo *et al.* (1998). The silicon antisite, Si_C, introduces a set of levels at about 0.2–0.4 eV above the top of valence band, for the charge states ranging from 4+ to 0. However, the carbon antisite, C_{Si}, does not introduce any states in the bandgap.

Several configurations of silicon and carbon interstitials (tetrahedral, hexagonal, and split-off) in 3C-SiC have been analyzed by Bockstedte and Pankratov (2000). They showed that all interstitial defects predominantly occur in positive charge states. The formation energy of Si_{TC}, about 1 eV, is almost 4 eV lower than that of any other interstitial of either type. For carbon interstitials, the energetically most favorable site is the split ⟨001⟩ position. So far, neither interstitials nor antisites have been positively identified in experiments.

Turning to group III nitrides, in the wurtzite structure there are two high-symmetry interstitial positions. The point symmetry is C_{3v} in both cases. The first site is located in the middle of the line connecting nonbonded gallium and nitrogen atoms, and has two

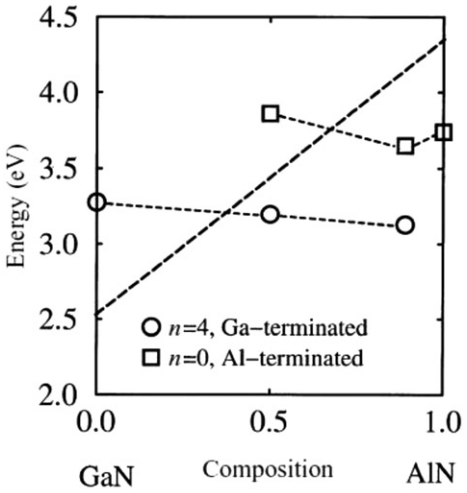

Fig. 3 Energy levels of V_N in GaN, AlN, $Al_{0.5}Ga_{0.5}N$, and $Al_{0.89}Ga_{0.11}N$ for $n=0$ aluminum-terminated (circles) and $n=4$ gallium-terminated (squares) variants. The dashed line is a linear interpolation of the theoretical bandgap. The dotted lines are only guides for the eye. After Bogusławski, P., Bernholc, J., 1999a. Doping and segregation effects in AlGaN systems. In: Liliental-Weber, Z., Miner, C. (Eds.), 1998 IEEE Semiconducting and Insulating Materials Conference 1999, pp. 233–238, New York, NY: IEEE Piscataway.

nearest neighbors and six next-nearest neighbors. The second site has six nearest neighbors. Bogusławski *et al.* (1995) found that the electronic structures and formation energies of both gallium interstitials are quite similar, despite the very different surroundings, and that they may act as compensating donors. Similar conclusions have been reached for aluminum interstitials in AlN. The formation energies of nitrogen interstitials are high and they should not be present in appreciable concentrations in either material. This holds also for antisites (partially owing to the large differences in atomic sizes between cations and nitrogen). Both Ga_N and N_{Ga} antisites introduce deep states close to the middle of the bandgap.

4 Irradiation and Defect Annealing in SiC

Annealing of defects in irradiated SiC has been studied by ESR and positron annihilation spectroscopy (PAS). The latter technique is well established for studies of vacancy-like defects in semiconductors, but it may only be used on *n*-type samples. (Otherwise the defects are positively charged and do not trap positrons.) Positron lifetime in bulk unirradiated SiC calculated by Brauer *et al.* (1996) agrees well with the experimental value measured by Polity *et al.* (1999). Brauer *et al.* (1996) also calculated the positron lifetime for V_C, V_{Si}, and a $V_C - V_{Si}$ divacancy for both cubic and hexagonal crystals. The differences between the polytypes are found to be minor, and the presence of vacancies increases the positron lifetime in each case. These results helped identify V_{Si}, divacancies, and vacancy clusters, and were used in studies of their annealing behavior (Kawasuso *et al.*, 1997; Brauer *et al.*, 1996).

The reduction of the defect concentration depends on the annealing temperature in a nonmonotonic fashion. Typically, a few characteristic temperatures ("stages") exist at which ESR and PAS spectra change; each indicates annealing of a specific type of defect. The progress of annealing depends on several parameters, such as the type of irradiating particles, their fluence, and the type of sample conductivity, since these factors determine defect concentrations and diffusivities.

According to Itoh *et al.* (1997), annealing of the silicon vacancy occurs at three stages, at about 150°C, 350°C, and 750°C, for both electron- and proton-irradiated *n*-type samples. Annealing at low temperatures is ascribed to the annihilation of vacancy–interstitial pairs, as suggested also by PAS experiments (Kawasuso *et al.*, 1997). In electron-irradiated *p*-type samples the ESR signal of V_{Si} disappears after an anneal at 350°C. The higher temperature stage is explained by the motion of vacancies, which are immobile at lower temperatures, towards extended defects like dislocations. Above 900°C, annealing of divacancies and dissociation of vacancy–impurity complexes takes place (Polity *et al.*, 1999). For high fluences, this picture is changed owing to the higher defect concentrations, and in particular to the presence of divacancies. Furthermore, the low-temperature stage is not observed in heavily irradiated specimens, which suggests that the concentration of close Frenkel pairs is low in this case.

The carbon vacancy is difficult to observe by PAS, possibly owing to insufficient trapping rate and its positron annihilation lifetime being similar to that of bulk crystal. ESR experiments indicate that the V_C^+ signal begins to decrease at 100°C, and vanishes after annealing at about 350°C. The annealing is due to the recombination with interstitial carbon rather than to the formation of $V_{Si} - V_C$ divacancies, since the latter are not seen in PAS.

After annealing at temperatures higher than 1450°C, the positron trapping is practically identical to that in unirradiated samples, indicating an almost complete anneal of irradiation defects.

In spite of considerable effort, the vacancies remain the only defects that have been identified thus far. Many other defect-induced levels have been observed and a few of them are tentatively attributed to native point defects. For example, Aboelfotoh

and Doyle (1999) suggest that the two levels at $E_c = -0.62$ eV and -0.64 eV, seen in their DLTS experiment in 6H-SiC *n*-type samples, are due to silicon vacancies and split by the hexagonal crystal field. They also propose that V_C introduces levels at -0.34 eV, -0.41 eV, and -0.51 eV below the conduction band. Itoh *et al.* (1997) suggested that T6 and T7 ESR-active states with effective spin $S=1$, which are created by electron irradiation, are Frenkel pairs (V_{Si}–Si(I) or V_C–C(I)). T6 and T7 disappear after anneal at 350°C in both proton- and electron-irradiated samples, which is similar to the annealing of V_C. This may support the notion of vacancy–interstitial annihilation.

5 Dopants in SiC

Nitrogen is the standard *n*-type dopant for SiC, and it is assumed to substitute for carbon. The donor energy, E_D, strongly depends on the polytype and on the type of site in a given polytype. In the 3C phase, E_D is 53 meV, and the effective mass theory provides an excellent description of the donor energies in both the ground and the excited states. In 6H-SiC, the donor energies are about 80 meV, 100 meV, and 125 meV, for the hexagonal (h) and the two quasi-cubic (k_1 and k_2) sites, respectively (Pensl and Chyoke, 1993). However, effective mass theory fails to describe accurately the nitrogen donor in both 4H- and 6H-SiC.

The most widely used acceptors are boron and aluminum. Boron acceptors have been studied in detail, since their properties are fairly complex. Two boron-related acceptor levels are observed, at about 0.3 eV and 0.6 eV above the top of the valence bands. It has been shown that the "shallow" boron-related level corresponds to off-center boron residing on a silicon site (Matsumoto *et al.*, 1997). The deep boron-related acceptor is a complex consisting of boron on the silicon site and a carbon vacancy (Gali *et al.*, 1999). Al_{Si} is the shallowest acceptor in SiC, with the acceptor energy of about 0.25 eV (depending on the lattice site and polytype).

6 Dopants in Group III Nitrides

We focus here on group IV dopants and selenium. Doping of GaN has been reviewed in detail by Pearton *et al.* (1999).

Both *n*- and *p*-type doping has been achieved in GaN and in $In_xGa_{1-x}N$ alloys over the whole composition range. However, doping of $Al_xGa_{1-x}N$ alloys becomes progressively more difficult with increasing aluminum content. In fact, the main problem preventing applications based on aluminum-rich $Al_xGa_{1-x}N$ alloys is the lack of effective dopants. Experimentally, the doping efficiency of silicon, which is the most widely used donor in group III nitrides, is quenched for aluminum content higher than about 0.5 (Bremser *et al.*, 1996; Stutzmann *et al.*, 1997; Skierbiszewski *et al.*, 1999). A similar effect is observed for *n*-type doping with germanium (Zhang *et al.*, 1995). A weaker decrease of hole concentrations with increasing aluminum content was reported for *p*-type doping with magnesium (Stutzmann *et al.*, 1997; Suzuki *et al.*, 1998; Katsuragawa *et al.*, 1998). These effects are partially explained by the fact that the ionization energies of dopants increase with increasing aluminum content, owing to an increase of the effective mass and a decrease of the dielectric constant. However, DX-center formation and self-compensation constitute more serious limitations of the doping efficiency.

Theoretical studies of group IV dopants have been carried out by Park and Chadi (1997); carbon, silicon, and germanium), Boguslławski and Bernholc (1997); carbon, silicon, and germanium). The particular focus of all these studies was the possible formation of DX centers and thus the quenching of the doping efficiency. However, the theoretical results are quite sensitive to the technical details of the calculations and differ significantly in some cases. For example, Boguslławski and Bernholc (1997) predict that in $Al_xGa_{1-x}N$ alloys grown in nitrogen-rich conditions and with $x<0.60$, Si_{cation} is an effective-mass donor; neither self-compensation nor the formation of NN pairs was expected (in spite of their relatively large binding energy, close to 1 eV). For alloys with $x>0.6$, their results suggest that a DX configuration is stable for the negatively charged silicon, which quenches the doping efficiency. Similar conclusions were reached for Ge_{cation}. In this case, efficient doping was predicted to occur only for $x<0.3$. For larger values of x, the doping efficiency is quenched owing to the stabilization of the DX^- state and appreciable self-compensation and pairing. However, Park and Chadi predict that germanium does not form a DX center and they predict a different geometry and energy for the silicon DX center. Finally, new calculations for AlN by Boguslławski, Briggs, and Bernholc (unpublished data, 1999c) that used a different computational method still find that silicon will form a DX center. Experimentally, the formation of a DX configuration for silicon was observed in $Al_xGa_{1-x}N$ for $x>0.5$ by Skierbiszewski *et al.* (1999) and Zeisel *et al.* (2000).

Carbon has been studied as a candidate acceptor that could potentially replace the commonly used magnesium. Experimentally, C_N in GaN is somewhat more shallow than magnesium (Fisher *et al.*, 1995) and leads to *p*-type conductivity in cubic GaN (Abernathy *et al.*, 1995), but not in wurtzite GaN (Birkle *et al.*, 1999). The latter negative result may possibly be due to the lack of gallium-rich growth conditions, which are necessary to effectively suppress self-compensation and pairing effects (Boguslławski and Bernholc, 1997). According to theory, C_N is an efficient acceptor for $Al_xGa_{1-x}N$ alloys in the cation-rich growth limit and for $x<0.4$. Calculations have also shown that C_{Ga} in the neutral and negative charge states is unstable on the substitutional site in $Al_xGa_{1-x}N$. It relaxes towards a DX configuration and becomes a deep donor.

As pointed out in Section 1, doping efficiency is also reduced by compensating native defects. Their formation energies are lowered by charge transfer effects and the energetic gain rises with increasing bandgap. Therefore, the degree of compensation by native defects in $Al_xGa_{1-x}N$ should increase with increasing aluminum content. This effect may be partially responsible for the

observed difficulties with *n*- and *p*-type doping. In the group III nitrides, the most important compensating donors are nitrogen vacancies and cation interstitials, while cation vacancies are compensating acceptors. For example, a high degree of compensation by gallium vacancies in GaN has been experimentally observed for Se_N donors (Yi and Wessels, 1996). In this case, the increased amount of compensation may be due to the formation of $Se_N - V_{Ga}^-$ NN pairs. The calculated binding energy of such pairs is large, 1.7 eV (Boguslławski and Bernholc, 1999b).

7 Interfacial Segregation

In heterostructures, such as GaN/AlN, the equilibrium concentration of dopants, given by Eq. (1), is in general different in the two constituents. One may thus expect interfacial segregation, i.e., diffusion of dopants across the heterointerface towards the constituent where the chemical potential of the dopant atoms is lower. Indeed, a change of the profile of the implanted impurities following annealing has been observed for various impurities in several heterojunctions (Hu *et al.*, 1991; Humer-Hager *et al.*, 1989; Moriya *et al.*, 1995). As discussed by Boguslławski and Bernholc (1999b), the difference between the chemical potentials can be approximated by the difference between the formation energies of impurities. This *segregation energy* determines the ratio of concentrations in the two constituents. For example, in the well-known case of Si/SiGe systems the concentration of boron is about twice as high in SiGe than in silicon, and the corresponding segregation energy is 0.3 eV.

Interfacial segregation in AlN/GaN heterostructures has been analyzed theoretically by Boguslławski and Bernholc (1999b). The calculated segregation energies of Se_N, C_N, and V_N are 0.95 eV, 1.2 eV, and 2.4 eV, respectively, which are all much larger than that of boron in Si/SiGe. Therefore, a pronounced interfacial segregation is expected and the equilibrium concentrations of these defects should be significantly lower in AlN than in GaN. However, the segregation energy of cation-substituting silicon is much lower, only 0.2 eV. This is because in the latter case the nearest neighbors of silicon (nitrogen atoms) are the same at both sides of the interfaces, while in the case of anion-substituting dopants the nearest neighbors of the impurity and thus the impurity–cation bonds are different, which significantly changes the total energy. For nitrogen vacancies, the interfacial segregation is another manifestation of the effect mentioned in Section 3, namely of the energetic preference of V_N for the gallium termination in $Al_xGa_{1-x}N$ alloys.

8 Current Trends in Analysis of Defects and Dopants in SiC and Group-III Nitrides

The possible mechanisms of silicon and carbon vacancy diffusion in cubic SiC are analyzed (Rurali *et al.*, 2003). The C vacancy can diffuse only by a direct migration of one of its second neighbors. Two mechanisms are possible for Si vacancy. It has been shown that even if Si vacancy encounters the lowest barrier in correspondence of the direct path, the first step of the indirect path is highly probable and will force most of the times the system to evolve through it. Even if the most favorable Minimum energy path corresponds to the diffusion of Si vacancy, its overall efficiency will be lowered by the parallel, indirect diffusion channel and the easiest diffusion will correspond to C vacancy.

A carbon vacancy defect is a point defect in SiC and of technological importance because the acceptor-like level of a carbon monovacancy (Z1/2 center: EC e 0.63 eV) works as the primary carrier-lifetime killer in 4HeSiC (Kimoto *et al.*, 2016). Low-energy electron irradiation or high-temperature treatment in an inert gas is essential for deliberate generation of carbon vacancy defects, though the depth profiles are different between the two The carbon vacancy defects can be removed to a deep region with a thickness of over 100 mm by either a Cþ implantation process or thermal oxidation. By combination of these processes, the density of carbon vacancy defects can be controlled. This can be directly linked to control of carrier lifetimes in SiC toward high-voltage bipolar devices.

The thermal evolution of defects produced in 4H–SiC by multiple implantation of C ions was examined by Low Temperature Photoluminescence in the temperature range 450–1000K (Litrico *et al.*, 2012). The photoluminescence spectra show sharp luminescent lines (alphabet lines) in the wavelength range 426–440 nm up on irradiation and thermal treatment at 450K. Up to 650K an annealing of defects involving both the alphabetic and the DI line occurs, while above 650K the alphabetic lines and the DI center show a different tendency with temperature. The alphabet lines intensity increases with temperature in the range 450–850K and then decreases with an activation energy of 2.0 eV owing to the related defect annealing. The Si-vacancy is proposed for the associated defect. The intensity of DI line increases in all the temperature range, nevertheless the increasing rate is higher from 650K. These increases are correlated to defects reconfiguration and to the annealing of carbon interstitial.

An overview of the historical background and the current issues of doping in III-nitride materials are provided (Pietro and Parbrooka, 2017). While doping of GaN is now well known and adequately controlled in standard optoelectronic devices, there is still a great deal of research on-going to improve the performance of advanced devices such as plasmonic sensors, or optical amplifiers. In AlN and high-aluminum-content AlGaN, on the contrary, it is very challenging to achieve a satisfactory doping level and ultraviolet-LEDs still suffer from a reduced wall-plug efficiency due to the poor conductivity of their cladding layers. Finally, in InN and high indium- content InGaN, stable control of the doping is even more difficult. Even though p-doping has been established, and InN nanowires have shown very appealing electrical characteristics, there are still no commercial devices available based on In-rich InGaN.

Group III-Nitrides receive much research attention and obtain remarkable development due to their wide applications in light emitting diodes, laser diodes, ultraviolet detectors, solar cells and field-effect transistors. Among the processes for III-nitrides

growth, molecular beam epitaxy provides its advantage in precise control of growth parameters, deep understanding of every growth step and in situ control of the growth. The recent progress of the growth of III-nitrides, the growth behavior, the effect of in situ monitoring on growth, the effect of polarity on III-nitrides and the doping, alloys and quantum structures of III-nitrides are demonstrated (Xinqiang and Yoshikawa, 2004).

Positron annihilation is an established technique for examining vacancy-type defects in semiconductors (Uedono *et al.*, 2009). When a positron is implanted into solids, it annihilates with an electron and emits two 511 keV γ quanta. From analysis of Doppler broadening spectra of the annihilation radiation and the positron lifetimes, vacancy-type defects such as mono-vacancies and divacancies can be detected. Monoenergetic positron beams are used to study vacancies in ion-implanted and rare-earth-doped GaN. The defect species are identified and their concentrations are estimated from a comparison between the Doppler broadening spectra obtained through the experiments and those calculated using first- principle calculation (projector augmented-wave method). Positron annihilation is a useful tool for studying relationships between vacancy-type defects and properties of group-III nitrides.

The growth, structural and optical properties of GaN/AlN Nano Wire heterostructures are investigated (Daudina *et al.*, 2012). It has been established that depending on In content, strain relaxation of InGaN grown on GaN NW may be elastic or plastic. Plastic strain relaxation has been noticed in the case of In-rich InGaN and is associated with formation of a relatively homogeneous alloy, with limited thermal delocalization of carriers. By contrast, In-poor alloy has been found to show elastic strain relaxation, partly assigned to strain-induced Ga and In segregation. Depending on their thickness and their In content, it is contemplated that InGaN quantum wells embedded in GaN barriers should also show clustering effect. This highlights the need for accurately controlling the In content in view of practical applications while recommending that the light emission variability of GaN/InGaN/GaN NW LEDs could be partly due to In concentration fluctuations. These fluctuations were found to be closely connected to the nature of the elastic strain relaxation process through the spontaneous formation of InGaN/GaN core/shell heterostructures.

Density functional theory computations was used to examine point defects of native species Zn_3N_2 and copper group elements Cu, Ag and Au (Nanke *et al.*, 2014). The formation energies of various native defects in Zn_3 N_2 and copper family were computed. The results show that Zn_3N_2 is a small bandgap material with a direct band transition behavior. The formation energies of both native defects and copper family impurities were affected significantly by the chemical potential of different atomic species. At a critical value of chemical potential of nitrogen, copper family favor nitrogen substitutional site. The electronic structure of copper doped Zn_3N_2 supports strong p type behavior while the doping of Ag or Au did not reveal such an effect.

9 Summary

Essential features of native defects and dopants in SiC and group III nitrides are discussed. In both SiC and group III nitrides, the only point defects clearly identified at present are the vacancies. The qualitative features of their electronic structure can be understood using a simple dangling-bond model introduced by Coulson. In group III nitrides, the nitrogen and cation vacancies are the main defects compensating intentional *p*- and *n*-type doping, respectively. Efficient dopants for SiC are well established, namely nitrogen for *n*-type and boron and aluminum for *p*-type. For GaN and $In_xGa_{1-x}N$, silicon and magnesium are the donor and the acceptor of choice. However, for aluminum-rich $Al_xGa_{1-x}N$ with x higher than about 0.5, efficient dopants are lacking. The observed strong reduction of doping efficiency is in part due to the increasing ionization energies of effective mass impurities. In the case of group IV dopants, however, both the DX center formation and self-compensation (owing to the incorporation of impurities on both sublattices) can strongly reduce the doping efficiency. Finally, interfacial segregation may have a considerable impact on the properties of group III nitride heterostructures.

Acknowledgment

This work was supported in part by KBN 2-P03B-093-14 and by the Office of Naval Research.

References

Abernathy, C.R., MacKenzie, J.D., Pearton, S.J., Hobson, W.S., 1995. CCl_4 doping of GaN grown by molecular beam epitaxy. Appl. Phys. Lett. 66, 1969–1972.
Aboelfotoh, M.O., Doyle, J.P., 1999. Defect energy levels in electron-irradiated and deuterium-implanted 6H silicon carbide. Phys. Rev. B 59, 10823–10829.
Bechstedt, F., Zywietz, A., Furthmuller, J., 1998. Carbon vacancy in SiC: A negative U system. Europhys. Lett. 44, 309–314.
Birkle, U., Fehrer, M., Kirchner, M.V., *et al.*, 1999. Studies of carbon as alternative p-type dopant for GaN. MRS. Internet J. Nitride Semicond. Res. [4S1 G5.6].
Bockstedte, M., Pankratov, O., 2000. Ab initio study of intrinsic point defects and dopant-defect complexes in SiC: Application to boron diffusion. Mater. Sci. Forum 338–342, 919–952.
Boguslławski, P., Bernholc, J., 1997. Doping properties of C, Si, and Ge impurities in GaN and AlN. Phys. Rev. B 56, 9496–9505.
Boguslławski, P., Bernholc, J., 1999a. Segregation effects at vacancies in AlGaN and SiGe alloys. Phys. Rev. B 59, 1567–1570.
Boguslławski, P., Bernholc, J., 1999b. Doping and segregation effects in AlGaN systems. In: Liliental-Weber, Z., Miner, C. (Eds.), 1998 IEEE Semiconducting and Insulating Materials Conference 1999, pp. 233–238, New York, NY: IEEE Piscataway.
Boguslławski, P., Briggs, E.L., Bernholc, J., 1995. Native defects in gallium nitride. Phys. Rev. B 51, 17255–17258.
Brauer, G., Anwand, W., Nicht, E.M., *et al.*, 1996. Evaluation of some basic positron-related characteristics of SiC. Phys. Rev. B 54, 2512–2517.

Bremser, M.D., Perry, G.W., Zheleva, T., *et al*., 1996. Growth, doping, and characterization of AlGaN thin film alloys on 6H-SiC (0001) substrates. MRS Internet J. Nitride Semicond. Res. 1 (1996), 8.
Chadi, D.J., Chang, K.J., 1988. Theory of the atomic and electronic structure of DX centers in GaAs and $Al_{1-x}Ga_xAs$. Phys. Rev. Lett. 61, 873–876.
Daudina, B., Bougerola, C., Camacho, D., *et al*., 2012. Growth, structural and optical properties of GaN/AlN and GaN/GaInN nanowire heterostructures. Phys. Proc. 28, 5–16.
Fisher, S., Wetzel, C., Haller, E.E., Meyer, B.K., 1995. On p-type doping in GaN – Acceptor binding energies. Appl. Phys. Lett. 67, 1298–1300.
Gali, A., Deak, P., Devaty, R.P., Choyke, W.J., 1999. Boron-vacancy complex in SiC. Phys. Rev. 60, 10620–10623.
Hu, M.S., Ahlgren, D.C., Ronsheim, P.A., Chu, J.O., 1991. Experimental study of diffusion and segregation in a Si/Si_xGe_{1-x} heterostructure. Phys. Rev. Lett. 67, 1450–1453.
Humer-Hager, T., Treichler, R., Wurzinger, P., Tews, H., Zwicknagl, P., 1989. Implantation-induced diffusion of Zn and B in GaAs/AlGaAs heterostructures. J. Appl. Phys. 66 (1989), 181–186.
Itoh, H., Kawasuso, A., Ohshima, T., *et al*., 1997. Intrinsic defects in cubic silicon carbide. Phys. Status Solidi A 162, 173–198.
Katsuragawa, M., Sota, S., Komori, M., *et al*., 1998. Thermal ionization energy of Si and Mg in AlGaN. J. Cryst. Growth 189–190, 528–531.
Kawasuso, A., Itoh, H., Ohshima, T., Abe, K., Okada, S., 1997. Vacancy production by 3 MeV electron irradiation in 6H-SiC studied by positron lifetime spectroscopy. J. Appl. Phys. 82, 3232–3238.
Kimoto, T., Kawahara, K., Zippelius, B., Saito, E., Suda, J., 2016. Control of carbon vacancy in SiC toward ultrahigh-voltage power devices. SuperlatticesMicrostruct. 99, 151–157.
Litrico, G., Zimbone, M., Musumeci, P., Calcagno, L., 2012. Defects annealing in 4H-SiC epitaxial layer probed by low temperature photoluminescence. Mater. Sci. Semicond. Process. 15, 740–743.
Look, D.C., Reynolds, D.C., Hemsky, J.W., *et al*., 1997. Defect donor and acceptor in GaN. Phys. Rev. Lett. 79, 2273–2276.
Matsumoto, T., Poluektov, O.G., Schmidt, J., Mokhov, E.N., Baranov, P.G., 1997. Electronic structure of the shallow boron acceptor in 6H-SiC: A pulsed EPR/ENDOR study at 95 GHz. Phys. Rev. B 55, 2219–2229.
Moriya, N., Feldman, L.C., Downey, S.W., King, S.A., Emerson, A.B., 1995. Interfacial segregation in strained heterostructures: Boron in $Si/Si_{0.8}Ge_{0.2}$. Phys. Rev. Lett. 75, 1981–1984.
Nanke, J., Roehl, J.L., Khare, S.V., Georgiev, D.G., Jayatissa, A.H., 2014. An ab initio computational study of pure Zn_3N_2 and its native point defects and dopants Cu, Ag and Au. Thin Solid Films 564, 331–338.
Park, C.H., Chadi, D.J., 1997. Stability of deep donor and acceptor centers in GaN, AlN and BN. Phys. Rev. B 55, 12955–13001.
Pearton, S.J., Zolper, J.C., Shul, R.J., Ren, F., 1999. GaN: Processing, defects, and devices. J. Appl. Phys. 86, 1–78.
Pensl, G., Chyoke, W.J., 1993. Electrical and optical characterization of SiC. Phys. B 185, 264–283.
Pietro, P., Parbrooka, P.J., 2017. Doping of III-nitride materials. Mater. Sci. Semicond. Process. 62, 180–191.
Polity, A., Huth, S., Lausmann, M., 1999. Defect characterization in electron-irradiated 6H-SiC by positron annihilation. Phys. Rev. B 59, 10603–10606.
Rurali, R., Hernandez, E., Godignon, P., Rebollo, J., Ordejon, P., 2003. First principles studies of neutral vacancies diffusion in SiC. Comput. Mater. Sci. 27, 36–42.
Skierbiszewski, C., Suski, T., Leszczynski, M., *et al*., 1999. Evidence for localized Si-donor state and its metastable properties in AlGaN. Appl. Phys. Lett. 74, 3833–3835.
Stutzmann, M., Ambacher, O., Cros, A., *et al*., 1997. Properties and applications of MBE grown AlGaN. Mater. Sci. Eng. B 50, 212–218.
Suzuki, M., Nishio, J., Onomura, M., Hongo, C., 1998. Doping properties and electrical characteristics of Mg-doped AlGaN grown by MOCVD. J. Cryst. Growth 189/190, 511–514.
Torpo, L., Nieminen, R.M., Laasonen, K.E., Poykko, S., 1999. Silicon vacancy in SiC: A high-spin state defect. App. Phys. Lett. 74, 221–223.
Torpo, L., Poykko, S., Nieminen, R.M., 1998. Antisites in silicon carbide. Phys. Rev. B 57, 6243–6246.
Uedono, A., Ishibashi, S., Ohdaira, T., Suzuki, R., 2009. Point defects in group-III nitride semiconductors studied by positron annihilation. J. Cryst. Growth 311, 3075–3079.
Wang, C., Bernholc, J., Davis, R.F., 1988. Formation energies, abundances, and the electronic structure of native defects in cubic SiC. Phys. Rev. B 38, 12752–12755.
Wimbauer, T., Meyer, B.K., Hofstaetter, A., Scharmann, A., Overhof, H., 1997. Negatively charged Si vacancy in 4H SiC: A comparison between theory and experiment. Phys. Rev. B 56, 7384–7388.
Xinqiang, W., Yoshikawa, A., 2004. Molecular beam epitaxy growth of GaN, AlN and InN. Progr. Cryst. GrowthCharact. Mater. 48/49, 42–103.
Yi, G.C., Wessels, B., 1996. Compensation of n-type GaN. App. Phys. Lett. 69, 3028–3030.
Zeisel, R., Bayerl, M.W., Goennenwein, S.T.B., *et al*., 2000. Phys. Rev. B 61, R16283–R16286.
Zhang, X., Kung, P., Saxler, A., *et al*., 1995. Growth of AlGaN:Ge on sapphire and silicon substrates. Appl. Phys. Lett. 67, 1745–1747.
Zywietz, A., Furthmuller, J., Bechstedt, F., 1998. Neutral vacancies in group IV semiconductors. Phys. Status Solidi B 210, 13–29.

Further Reading

Dongjin, W., Redwing, J.M., 2013. Effect of AlN bufferlayers on the surface morphology and structural properties of N-polar GaN films grown on vicinalC-faceSiC substrates. J. Cryst. Growth 377, 51–58.
Hang, Z., Jiang, W., Liu, W., *et al*., 2016. Vacancy effects on the formation of He and Kr cavities in 3C-SiC irradiated and annealed at elevated temperatures. Nucl. Instrum. Methods Phys. Res. B 389–390, 40–47.
Mohd, I.I., Yamazaki, S., Yoshida, K., Yano, T., 2016. Defects annihilation behavior of neutron-irradiated SiC ceramics densified by liquid-phase-assisted method after post-irradiation annealing. Nucl. Mater. Energy 9, 199–206.
Neugebauer, J., Van de Walle, C.G., 1994. Atomic geometry and electronic structure of native defects in GaN. Phys. Rev. B 50, 8067–8071.
Petrenkoa, T.T., Petrenkoa, T.L., Bratus'a, V.Ya., Monge, J.L., 2001. Symmetry, spin state and hyperfine parameters of vacancies in cubic SiC. Appl. Surf. Sci. 184, 273–277.
Richter, E., Gridneva, E., Weyers, M., Tränkle, G., 2016. Fe-doping in hydride vapor-phase epitaxy for semi-insulating gallium nitride. J. Cryst. Growth 456, 97–100.
Van de Walle, C., 1998. DX-center formation in wurtzite and zinc blende $Al_xGa_{1-x}N$. Phys. Rev. B 57, R2033–R2036.
Zhuang, D., Edgar, J.H., 2005. Wet etching of GaN, AlN, and SiC: A review. Mater. Sci. Eng. R 48, 1–46.
Zolper, J.C., 1997. Ion implantation in group III nitride semiconductors: A tool for doping and defect studies. J. Cryst. Growth 178, 157–167.